ST-18

Mathematical Modeling for Prediction of Intracranial Pressure with Non-Invasive Methods based on Intraocular Pressure, Cerebral Perfusion Pressure, and Mean Arterial Blood Pressure

Kritchanan Charoensuk[1] and Kanchit Pawananont[2]

[1] Faculty of Engineer, Department of Mechanical Engineering, BangkokThonburi University
[2]Faculty of Engineering and Industrial Technology, Department of Robots and Smart Electronics Engineering, Phetchaburi Rajabhat University
Email: C.kritchanan@gmail.com

Abstract

In this study, the mathematical modelling of various systems, including intracranial pressure (ICP), cerebral perfusion pressure (CPP), intraocular pressure (IOP), and mean arterial pressure (MAP), is studied based on the 3D-Paraboloid and 3D- Gaussian mathematical model. Healthy and unhealthy people from clinical data are used to study those behaviours. The clinical data from examined and article has constructed a relationship of 3D locus, which included ICP inside the skull, IOP of the retinal vessel, CPP in the skull. Moreover, the coefficient of determination is applied to this mathematical modelling for synchronized healthy and unhealthy data. The results show that the 3D locus value of ICP of the normal and abnormal state, IOP, and CPP in the skull are 5-15 mmHg, 20-35 mmHg, and 65-90 mmHg, respectively. For the relationship in the 3D locus between MAP, CPP, IOP, and ICP 3D-Gaussian mathematical model giving r-squared values are 0.97 in the MAP-CPP-ICP case and 0.94 in the MAP-IOP-ICP and the 3D-Paraboloid mathematical model are 0.89 in the MAP-CPP-ICP case and 0.78 in the MAP-IOP-ICP. The 3D-Gaussian mathematical model gave accuracy higher than the 3D-Paraboloid mathematical model. Finally, Clinical data from non-invasive measuring methods verify our model. This model clarifies healthy individuals' interaction behaviour between ICP, CCP, IOP, and MAP.

Keywords: intracranial pressure; 3D- Gaussian mathematical; non-invasive; 3D locus ;

Introduction

Nowadays, human diseases in the brain are one of the most disastrous health problems in industrialized nations (Barry R. Bloom, 2006.)Transient Global Amnesia (TGA)(C. -P. Chung et al., 2006; D Owen, B Paranandi, R Sivakumar, & Seevaratnam, 2007), Transient Monocular Blindness (TMB) including blindness (C.Y. Cheng, F.C. Chang, A.C. Chao, C.P. Chung, & H.H. Hu, 2013), and Parkinson's disease are a neurodegenerative disorder of the central nervous system and effects in people older than 50 years of age. The symptoms include shaking, rigidity, difficulty with walking, depression, speech, and cognitive and emotional problems(Manju Liu et al., 2015). ICP is a critical parameter for diagnosing the neurosurgical condition, traditionally detected by an invasive method. The invasive measurement of ICP was a popular measuring method in the current clinical. The diagnosis result from invasive equipment gives higher precision than noninvasive that was reported by H. Cushing (Avolio, 1980), O. Gilland et al. (Gilland, 1969). (7), and M.smith et al.(M. Smith, 2008). The human immune mechanism would obtain practical tools or tissue to replace the wound by installing invasive equipment. The alternative to investigating the disease of the human brain is noninvasive equipment. For example, the ultrasound signals to measure cerebral blood flow velocity (CBFV) indices(P. R. Hanlo P et al., 1995), skull vibrations (Ueno T, 1998)(, brain tissue resonance (D, 2002), or transcranial time-of-flight (D, 2002; R. V. D. G. Ragauskas A, Pektus V., 2003), venous ophthalmology-manometry (L. P. Querfurth H, 2010), optic nerve sheath diameter assessment (M. L. Borchert, 1998), sensing tympanic membrane displacement (M. R. Reid A, 1989), analyzing otoacoustic emissions (A. C. Frank A, 2000), magnetic resonance imaging to estimate incremental intracranial compliance (L. S. Alperin N, 2000), and recordings of visual evoked potentials (Z. J. Zhao Y, 2005). Also, the approach described by Ragauskas et al.(D. A. D. G. Ragauskas A, Azelis V, Gedrimas V., 2005) applied external pressure on the eyeball to balance the flow characteristics in the internal and extracranial segments of the ophthalmic artery. The balance condition was detected by a two-depth transcranial Doppler (TCD) ultrasound, and the corresponding external pressure was taken as the IOP evaluation. The ICP result was created and mapped with MAP, IOP, and multi-parameter to generate from their method(Toro., 2016). The IOP value of optic nerve is showing not only to IOP in the eye, but also to intracranial pressure (ICP), as it is surrounded by cerebrospinal fluid (CSF) in the subarachnoid space. The lamina cribrosa separate these two pressurized regions and the pressure drop that occurs across the laminacribrosa is known as the translaminar pressure difference and is typically directed posteriorly. Recent data indicate that ICP is lower in patients. The ICP value from the noninvasive method gives lower accuracy than the invasive method. Because of noninvasive methods use the third parameter, such as BP, IOP, and CCP for calculating ICP. A large number of parameters and the lack of an underlying mechanistic model mean that such "black box" mappings can fail to adequately and robustly capture the relevant physiology.

The mathematical model can improve the precision of noninvasive methods in which the relationship of ICP, CPP, IOP, and MAP is investigated by assessing the mechanical action of the heart and spinal cord on clinically measurable hemodynamic quantities of MAP and CSF pressure in the skull and spinal cord are applying to the

mathematical model. Over the past decade, the logic of models developed by modelling such a critical system has become a valuable tool for diagnosing diseases and recommending the appropriate way of their medical treatment. Moreover, M. Czosnyka et al. (Marek Czosnyka, 1997) developed the models of the brain's mechanic-elastic properties that were related to the CSF circulation and included the non-linear pressure-volume relation of the intracranial compartment. The relation of CSF and MAP is directly affected by ICP value, shape of amplitudes, and offset range diagram; thus, the circumstance shows the same behaviour of CSF, MAP, and ICP. These studies laid the foundation for techniques used to diagnose hydrocephalus and tumour. The Advances in computing technology have prompted attempts to integrate the intracranial CSF circulation with CBF.

Furthermore, the IOP has used predicted behaviour of ICP when lamina cribrosa is considered the anatomic landmark of interest in healthy conditions and other diseases where IOP and ICP are important contributory factors. As mentioned earlier, at any known moment, the lamina cribrosa is under the control of two-part but possibly mutually supporting pressures – the following acting IOP and the anteriorly substitute ICP. The circumstances between ICP and IOP were proved in simulation and the experimental, which were reported and analyzed by U.R. Chowdhury and M. P. Fautsch (Chowdhury & Fautsch, 2015) and F.David et al.(Werndle MC, 2014)

In this paper, the model-based approach to obtaining estimates of the principal locus of the human body, which is predicted in an average human by rain, blood, and body fluids (Cerebrospinal fluid, retinal fluid, etc.) of the human body that includes healthy cases and unhealthy cases from noninvasive waveform measurements of intracranial pressure (ICP), cerebral perfusion pressure (CPP), intraocular pressure (IOP), and arterial blood pressure (MAP). The mathematical model will develop to increase the performance of noninvasive methods. Our approach does not require patient-specific calibration or training on a reference population. The associated computational burden is negligible, allowing the near-real-time estimation of human body behaviour.

Purposes

1) To study and understand the relationship between intracranial pressure (ICP), cerebral perfusion pressure (CPP), intraocular pressure (IOP), and mean arterial pressure (MAP)

2) The intracranial pressure (ICP) behaviour can be predicted from Non-Invasive Methods based on the mathematics model.

Research Methodology

This work aimed to determine the principal locus for the brain, blood, and body fluids (Cerebrospinal fluid, retinal fluid, etc.) of the human body, including healthy cases and unhealthy cases hybrid approach between critical data and mathematical equation. At this moment, the behaviour of intracranial pressure (ICP), cerebral perfusion pressure (CPP), intraocular pressure (IOP), and arterial blood pressure (MAP) were taken into account. The critical data of each case with continuous recording and medical literature are supplemented by other modalities, including MAP (in all cases), CPP (in all cases), IOP(recorded intermittently in ~ 45% of all cases), and ICP (recording ~ 35 % and using ICP formula~ 65% of all cases). The study population included teenage and adult patients aged 17 to 85 years (average age of 35 years). All patients have different treatment regimens and protocols used within this period, beginning with treatment without any fixed treatment. To generate principal locus of the human body obtained from clinical data using ICP-time, MAP-time, CPP-time, and IOP-time. Clinical parameters of ICP, MAP, CPP, and IOP for evaluating human body locus were reported for healthy cases and unhealthy points; thus, the data of creating the 3D-locus are included in the report of doctors and researchers who work in this field from the medical literature(A. C. Frank A, 2000; C. -P. Chung et al., 2006; D. A. D. G. Ragauskas A, Azelis V, Gedrimas V., 2005; R. V. D. G. Ragauskas A, Pektus V., 2003; L. S. Alperin N, 2000; Morgan William H. MBBS & Yu Dao Yi, 2008; Z. J. Zhao Y, 2005). From each relation, the relations were transformed into the principal locus of the human body. Thus, the mathematical equations were used to obtain the 3-D principal locus of the human body to interpret the clinically measured hemodynamic response to treatment ICP reduction in brain condition patients and ICP elevation in healthy individuals. The mathematical model in this work has composed of two equations. The first one is that the 3D-Paraboloid equation thus was used and applied in the research of so S. Badri et al.(Shide Badri et al., 2012). Furthermore, David W. Smith et al.(D. W. Smith, , , & 2019), the equation can express in equation (1).

$$z = c_0 + p_1 x + p_2 y + p_3 x^2 + p_4 y^2 \quad (1)$$

P1, P2, P3, and P4 are constant values of the 3D-Paraboloid equation, and C0 represents the limit of the 3D boundary on the z-axis. Next, the second part is the 3D-Gaussian equation presented by Faisal M. Kashif et al.(Faisal M. Kashif, George C. Verghese, Vera Novak, Marek Czosnyka, & Heldt, 2012). The equation can express in equation (2).

$$z = G_1 e^{0.5\left[\left(\frac{x-G_4}{G_2}\right)^2+\left(\frac{y-G_5}{G_3}\right)^2\right]} \quad (2)$$

Where G1, G2, G3, G4 and G5 are constant values of the 3D-Gaussian equation. x0 and y0 represent the limit of the 3D boundary on the x-axis and y-axis. Equations (1) and (2) were used for generating the principal locus of the human body, and constant parameters can present relation among ICP, MAP, CPP, and IOP. Likewise, the amplitude and behaviour of each result were supported by clinical data. Finally, the human body's principal locus was used to evaluate ICP behaviour and diagnose clinical data brain disease via recorded data and medical literature.

Results

In our recent publication, the human body's principal locus was generated to represent the behaviour of ICP, CCP, MAP, and IOP of the human body. The ICP, CPP, MAP, and IOP obtained from clinical data and the medical literature was correlated to each other, and moments of abnormal conditions were evaluated. The value, the healthy, and abnormal conditions were collected, which are reported in Tables 1 and 2. The value of ICP, CPP, MAP, and IOP clearly shows the difference in their value, so the 3D locus can explain each parameter's behaviour and predict the ICP value from the 3D locus of the human body. The relationship of content will be explained in the next section.

The first result, ICP, is composed of blood, body fluids (Cerebrospinal fluid, retinal fluid, etc.) and brain tissue. Thus, this research was ingrained into the effect of brain tissue. The constant parameter of the 3D locus of the human Diagrams is computed from ICP-time, MAP-time, CPP-time, and IOP-time and medical literature. The 3D equation for generating has 3 D-Paraboloid and 3 D- Gaussian mathematical equations and has two groups of relationships among ICP, MAP, and CPP for the first section and ICP, MAP, and IOP for the second group. The first and second groups of 3D locus of the human diagrams were verified from clinical data and created from 3D-Paraboloid and 3D- Gaussian. The 3D locus of ICP, CPP, IOP, and MAP shows healthy and unhealthy data in the 3D-Paraboloid equation and 3D-Gaussian model, as shown in Fig 1 and 2. Figures 1 and 2 show the relationship between ICP, MAP, IOP, and CPP, displaying the boundary between healthy and unhealthy conditions. The 3D-locus of the Paraboloid model in Fig. 1a. and 2a. has included The unhealthy and healthy conditions examined from 34 patients who have brain desires such as stroke, tumour, and high pressure. The ICP value has between 40-70 mmHg, which means the effect of ICP will be disturbed blood circular. The CCP value is between 30-50 mmHg, and the MAP value is over 120 mmHg.

Meanwhile, the ICP, CCP, and MAP value's healthy condition is 5-15 mmHg, 60-90 mmHg, and 85-110 mmHg, respectively, which has been examined from ordinary people, including 37 persons in adults and teen. Moreover, the IOP value was considered for diagnosing the ICP value to replace the CPP value, while the relative relationship among MAP, IOP, and ICP was created. The IOP value has included 27 patients, 10 cases were gluten, and 17 cases were stroke. The healthy case has 26-28 mmHg, and the unhealthy case has over 32 mmHg. From clinical data in an unhealthy and healthy case, the constant value in the 3D-Paraboloid equation and R-squared in table 1. In Figures 2b. and 2b., the 3D locus of the Gaussian model, the relationship among ICP, MAP, IOP, and CPP, shows an extract boundary between healthy and unhealthy conditions, mainly from the prevision section. The unhealthy condition was examined in 34 patients with brain desires such as stroke, tumour, and high pressure. The ICP value has between 40-70 mmHg, which means the effect of ICP will be disturbed blood circular. The CCP value is between 30-50 mmHg, and the MAP value is over 120 mmHg. Meanwhile, the ICP, CCP, and MAP value's healthy condition is 5-15 mmHg, 60-90 mmHg, and 85-110 mmHg, respectively, which has been examined from ordinary people, including 37 persons in adults and teen. From calculated data in an unhealthy and healthy case, the constant value in the 3D- Gaussian equation and R-squared value are shown in table 2. From tables 1 and 2, the 3D- Gaussian

equation gives a higher value of R-squared value than the 3D- Paraboloid equation. The same conditions were reported by U. Farooq et al. (41) (Umar Farooq, Jason Gu, Mohamed E. El-Hawary, Jun Luo, & Asad, 2015) explained in a scientific model and computational structure for the determination. The 3D- Gaussian equation explained a microfluidic device's 3D functional human microvascular network. This model enables human vascular endothelial cells to form tissue-like microvessels that perform very equally to human blood vessels reported by Y. li et al.(D. W. Smith et al., 2019) (. The 3D- Gaussian equation used predicted the relationship between ICP, MAP, IOP, and CPP in this paper. The relation of the 3D equation's clinical date parameters can express in equation (3).

$$ICP = 71.192 \cdot e^{\left(-05 \cdot \left(\left(\frac{MAP-154.625}{69.042}\right)^2 + \left(\frac{CPP-22.596}{22.886}\right)^2\right)\right)} \quad (3)$$

Moreover, the doctor considered the IOP value for diagnosing the ICP value to replace the CPP value. Simultaneously, the relative is the relationship between MAP, IOP, and a mathematical equation created by ICP. The IOP value has included 27 patients, 10 cases were glaucoma, and 17 were strokes. The healthy case has 26-28 mmHg, and the unhealthy case has over 32 mmHg. The equation can express in equation (4).

$$ICP = 89.161 \cdot e^{\left(-05 \cdot \left(\left(\frac{MAP-134.176}{53.062}\right)^2 + \left(\frac{IOP-43.512}{10.382}\right)^2\right)\right)} \quad (4)$$

From equations (3) and (4), the ICP value can calculate and compare with Clinical data from non-invasive measuring methods to verify our model. This model clarifies healthy individuals' interaction behaviour between ICP, CCP, IOP, and MAP. The relation and behaviour of their model will explain in the section.

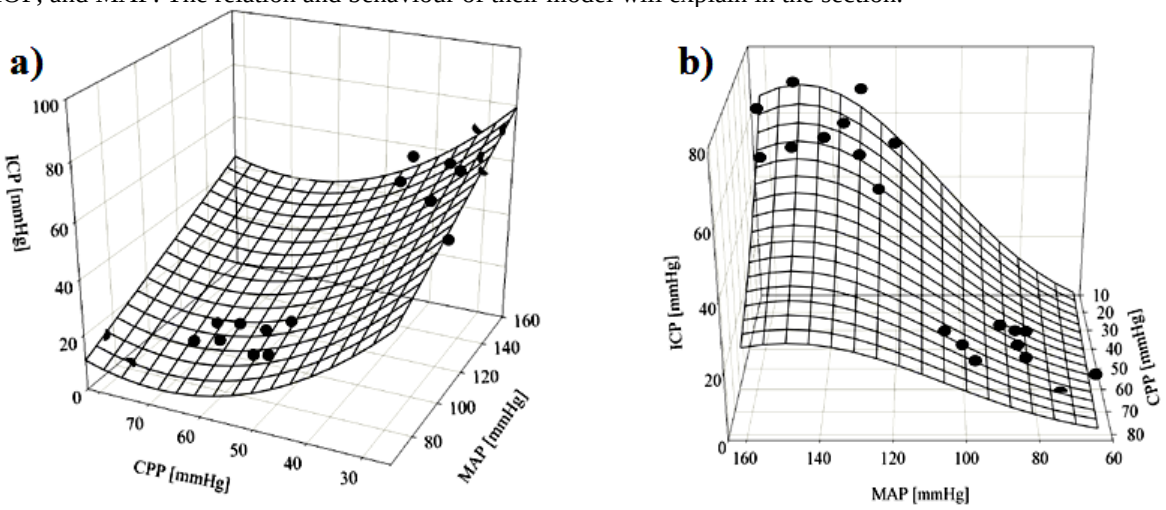

Fig. 1. 3D locus of MAP, CPP, and ICP in a)3D-Paraboloid model and b) 3D-Gaussian model

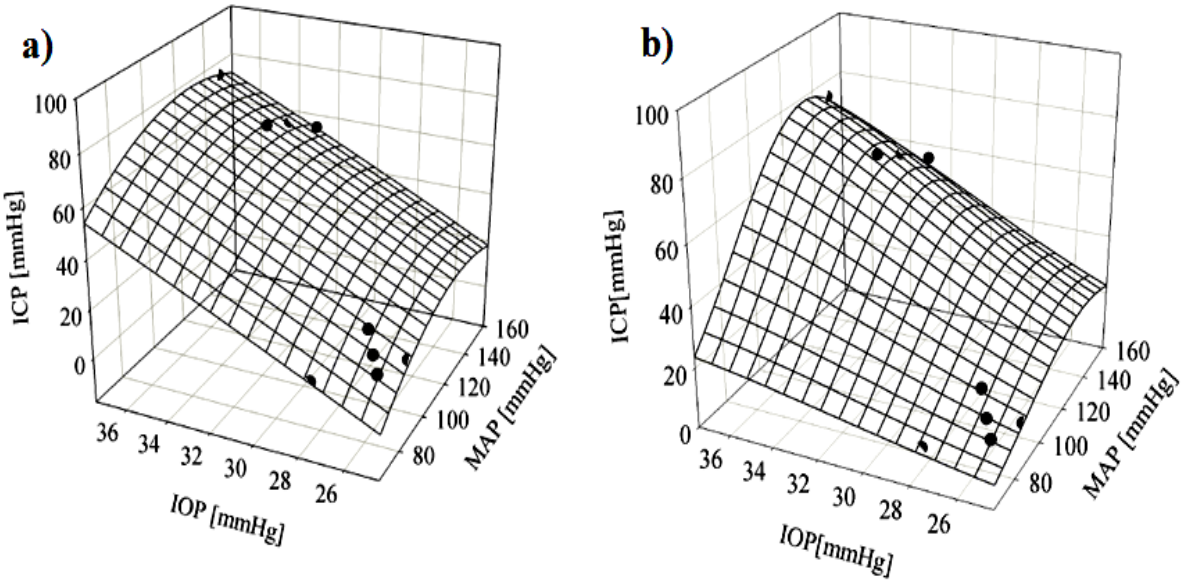

Fig. 2. 3D locus of MAP, IOP, and ICP in a) 3D- Paraboloid model and b) 3D- Gaussian model

Discussion

The results of the 3D locus of the human base on clinical data and examined from patients, the verified data of critical cases from the article and examined data were performed on the 3D locus in healthy and unhealthy zone, as shown in Fig. 3. The verified data was focused on vascular diseases in the brain and the eyes, which have a tumours, stroke, hypertension, and glaucoma. It is seen that the data from critical cases from the article and examined data were commonly observed at the 3D locus. Additionally, the verified data was used in both the 3D loci of the human in the 3D-Paraboloid mathematical model and the 3D- The gaussian mathematical model. The clinical data determined ICP, CCP, MAP, and IOP on the vascular in the brain and eye in unhealthy cases and examined data in the healthy case until unhealthy cases were plotted on the 3D locus, as illustrated in Fig. 3a and 3b for the 3D-Paraboloid and3D-Gaussian mathematical model, respectively.

Table 1. The constant value of the 3D locus of MAP, CPP, IOP, and ICP in the Paraboloid model

Condition	P_1	$_2P$	$_3P$	P_4	r-squared value
MAP-CPP-ICP	-19.43	0.016	0.572	-0.006	0.78
MAP-IOP-ICP	-19.92	0.2	0.743	0.009	0.89

Table 2. The constant value of the 3D locus of MAP, CPP, IOP, and ICP in the Gaussian model

Condition	G_1	$_2G$	$_3G$	G_4	G_5	r-squared value
MAP-CPP-ICP	147.67	20.75	60.04	30.27	23.89	0.97
MAP-IOP-ICP	180.29	32.78	86.91	-45.13	11.89	0.94

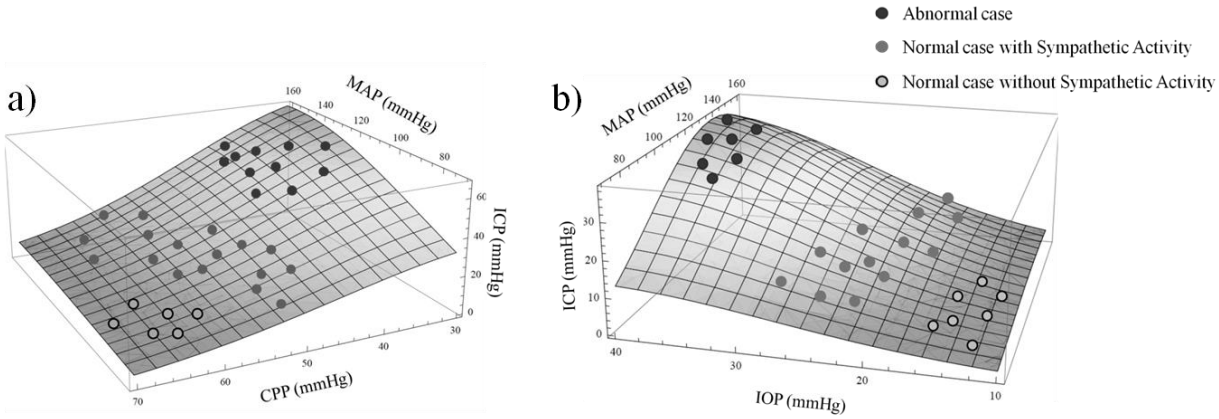

Fig. 3 a) 3D locus of MAP, CCP, and ICP b) MAP, IOP, and ICP in 3D- Gaussian *model with verified data.*

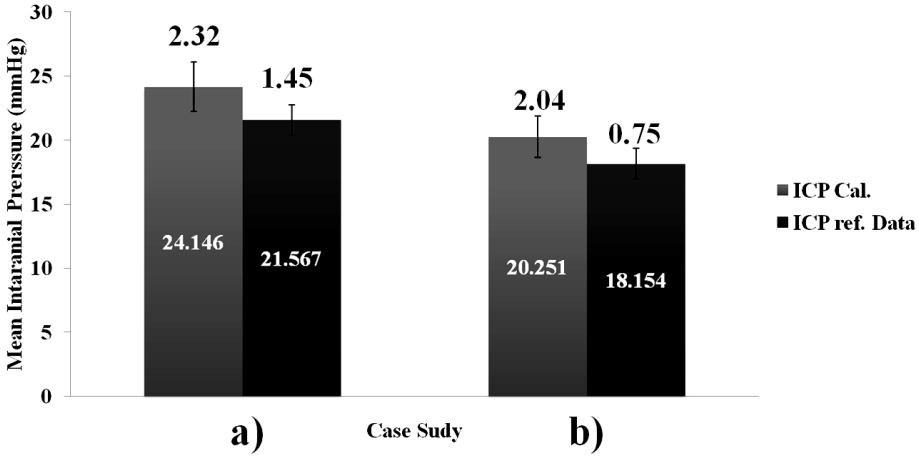

Fig. 4 ICP comparison based on a) CCP and b) IOP in 3D- Gaussian *model*

Conclusion

The 3D locus was created as the 3D-Gaussian mathematic model for investigating ICP, CPP, IOP, and MAP in the brain system in healthy people's reasonable conditions. The relation between blood, cerebrospinal fluid, the eye, and the brain was determined to follow the mathematic model; thus, the 3 D locus includes the 3 D-Gaussian and clinical data. Moreover, the results show the following:

- The determination of the 3D locus of the human for healthy and unhealthy people shows that the r-squared value of 3 D- Gaussian is higher than a 3 D-Paraboloid mathematical model. the value was shown in table 1 and 2 . These results were supported by clinical data, which have the confidant level index of 0.95.

- the ICP of healthy and un unhealthy people was calculated in the clinical data and then compared with those redacted by the reference data based on clinical data, as shown in Fig.4 for the examined data. In addition, calculated ICP at the normal case and abnormal states were evaluated and provided. It is seen that the used 3D- Gaussian models significantly affected the predicted ICP. These results were supported by clinical data, which have the confidant level index of 0.95.

Additionally, the predicted value of ICP, CPP, IOP, and MAP in this model was supported by the clinical data from the noninvasive measuring method. Moreover, this model also clearly explains the behaviour interaction between ICP, CCP, IOP, and MAP of healthy people.

References

A. C. Frank A, H. P., Janssen T, Arnold W, Trappe A. (2000). Noninvasive measurement of intracranial pressure changes by otoacoustic emission (OAEs) – *a report of preliminary data. Zentralbl Neurochir*, 61, 177-180.

Avolio, A. (1980). *Multi-branched model of the human arterial system*. Medical & Biological engineering & Computing, 709-718.

Barry R. Bloom, C. M. M., John R. La Montagne, and others. (2006.). *Disease Control Priorities in Developing Countries (C. M. M. Barry R. Bloom, John R. La Montagne, and Lone Simonsen. Ed.)*. New York: Oxford University Press.

C. -P. Chung, H. -Y. Hsu, A. -C. Chao, F. -C. Chang, W. -Y. Sheng , & Hu, H.-H. (2006). Detection of intracranial venous reflux in patients of transient global amnesia. *Neurology, 66*(12), 1873-1877.

C.Y. Cheng, F.C. Chang, A.C. Chao, C.P. Chung, & H.H. Hu. (2013). Internal jugular venous abnormalities in transient monocular blindness. *BMC Neurology*, *13*(94), 1417-2377.

Chowdhury, U. R., & Fautsch, M. P. (2015). Intracranial Pressure and Its Relationship to Glaucoma: Current Understanding and Future Directions. Roy Chowdhury U, Fautsch MP. Intracranial Pressure and Its Relationship to Glaucoma: Current Understanding and Future Directions. *Med Hypothesis Discov Innov Ophthalmo*l. 2015;*4*(3):71-80.

D Owen, B Paranandi, R Sivakumar, & Seevaratnam, M. (2007). Classical diseases revisited: transient global amnesia. *Postgraduate Medical Journal*, *83*(978), 236-239.

D, R. Z. M. (2002). Tissue resonance analysis; a novel method for noninvasive monitoring of intracranial pressure. *Journal of Neurosurger, 96*, 1132-1137.

D. G. Ragauskas A, D. A., Azelis V, Gedrimas V. (2005). Innovative non-invasive method for absolute intracranial pressure measurement without calibration. (Acta Neurochirurgica Supplements): Springer.

D. G. Ragauskas A, R. V., Pektus V. (2003). Implementation of noninvasive brain physiological monitoring concepts. *Medical Engineering & Physics, 25*(676-678).

Faisal M. Kashif, George C. Verghese, Vera Novak, Marek Czosnyka, & Heldt, T. (2012). Model-Based Noninvasive Estimation of IntracranialPressure from Cerebral Blood Flow Velocityand Arterial Pressure. *Science translational medicine, 4*, 1-9.

Gilland, O. (1969). Normal cerebrospinal-fluid pressure. England Journal of Medicine, 280(16), 904-905.

L. P. Querfurth H, A. S., Mundell S, Bennett M, van Horne C. . (2010). Opthalmodynamometry for ICP prediction and pilot test on Mt. *Everest. BMC Neurology, 10*, 106.

L. S. Alperin N, L. F., Raksin P, Lichtor T.,. (2000). MR-Intracranial pressure (ICP): a method to measure intracranial elastance and pressure noninvasively by means of MR imaging: baboon and human study. *Radiology*, 177-180.

M. L. Borchert, J. (1998). *Non-invasive method of measuring cerebrospinal fluid pressure*.

M. R. Reid A, B. D., Martin A, Brightwell A, Pickard J. (1989). Mean intracranial pressure monitoring by a non-invasive audiological technique: a pilot study. *Journal of Neurology, Neurosurgery, and Psychiatry, 52*, 610-612.

Manju Liu, Haibo Xu, Yuhui Wang, PhD, Y. Z., Shuang Xia, David Utriainen, . . . E. Mark Haacke. (2015). Patterns of chronic venous insufficiency in the dural sinuses and extracranial draining veins and their relationship with white matter hyperintensities for patients with Parkinson's disease. *Journal of Vascular Surgery, 61*(6), 1511-1520.

Marek Czosnyka, S. P., Hugh K Richards, Peter Kirkpatrick, Piotr Smielewski, and J. D. Pickard. (1997). Contribution of mathematical modelling to the interpretation of bedside tests of cerebrovascular autoregulation. Journal of Neurology, *Neurosurgery, and Psychiatry, 63*, 721-731.

Morgan William H. MBBS, & Yu Dao Yi. (2008). The Role of Cerebrospinal Fluid Pressure in Glaucoma Pathophysiology: The Dark Side of the Optic Disc. *Journal of Glaucoma, 17*(5), 408-413.

P. R. Hanlo P, Gooskens R, Heethaar R, Keunen R, v., Huffelen A, Tulleken C, & J., W. (1995). Monitoring intracranial dynamics by transcranial Doppler --- a new Doppler index: trans systolic time. *Ultrasound Med and Bio, 21*, 613-621.

Shide Badri, Jasper Chen, Jason Barber, Nancy R. Temkin, Sureyya S. Dikmen, Randall M. Chesnut, . . . Treggiari, M. M. (2012). Mortality and long-term functional outcome associated with intracranial pressure after traumatic brain injury. *Intensive Care Medicine, 38*, 1800-1809.

Smith, D. W., , C.-J. L., , W. M., & , B. S. G. (2019). Estimating three-dimensional outflow and pressure gradients within the human eye. PLoS ONE, 4, 1-45. doi:https://doi.org/10.1371/journal.pone.0214961

Smith, M. (2008). Monitoring intracranial pressure in traumatic brain injury. *Anesthesia and Analgesia, 106*(1), 240-248.

Toro., E. F. (2016). Brain venous haemodynamics, neurological diseases and mathematical modelling. *A review. Applied Mathematics and Computation, 272*, 542-579.

Ueno T, B. R., Shuer L, Cantrell J, Yost W. (1998). Noninvasive measurement of pulsatile intracranial pressure using ultrasound. *Acta Neurochirurgica Supply, 71*, 66-69.

Umar Farooq, Jason Gu, Mohamed E. El-Hawary, Jun Luo, & Asad, M. U. (2015). *Observer based fuzzy LMI regulator for stabilization and tracking control of an aeropendulum*. Paper presented at the IEEE 28th Canadian Conference on Electrical and Computer Engineering (CCECE).

Werndle MC, S. S., Phang I, Czosnyka M, Varsos GV,Czosnyka ZH. (2014). Monitoring of spinal cord perfusion pressure in acute spinal cord injury: initial findings of theinjured spinal cord pressure evaluation study. *Critical Care, 42*, 646–655.

Z. J. Zhao Y, Z. G. (2005). *Clinical experience with the noninvasive ICP monitoring system.: Springer*.